Clays and Clay Minerals, Vol. 39, No. 6, 622–633, 1991.

CHLORITE VERMICULITIZATION AND PYROXENE ETCHING IN AN AEOLIAN PERIGLACIAL SAND DUNE, ALLEN COUNTY, INDIANA

SCOTT ARGAST

Department of Geosciences, Indiana University-Purdue University at Fort Wayne
Fort Wayne, Indiana 46805-1499

Abstract—Weathering has etched and deeply-denticulated the constituent orthopyroxenes, and chlorite has been transformed to vermiculite in the upper 3 m of an aeolian, periglacial sand dune formed in northeastern Indiana about 13,000 b.p. Pyroxene weathering begins with the development of cleavage-parallel etch pits on {010} and {100} surfaces. These pits coalesce and eventually crop out on basal surfaces as denticulations. The mean denticulation size increases logarithmically toward the surface, and the denticulation size of the orthopyroxenes is a quantifiable feature of the weathering process. Ferruginous pendants, microboxworks of iron oxides, and other indications of iron redeposition within the orthopyroxene microenvironments were not observed.

Chlorite in the dune has been weathered to vermiculite. The parent chlorite is a high-Fe variety, and the transformation to vermiculate does not involve the development of a chlorite/vermiculite intermediary phase. Fe^{2+} is oxidized as part of the transformation process and this iron is retained in the sediment as discrete goethite and as crystalline and noncrystalline coatings on the dune grains. The vermiculite from depths shallower than 64 cm is only partly expandable and is completely collapsed by K-saturation or heat treatment. This is a hydroxy-Al vermiculite and its formation is typical of intense weathering under the acid conditions prevalent at the dune surface.

Key Words—Chlorite, Denticulations, Dunes, Etching, Hydroxy-Al, Indiana, Pleistocene, Pyroxene, Vermiculite, Weathering.

INTRODUCTION

Pyribole weathering is a process affecting the geochemical cycles of Si, Al, Fe and Mg. It was once suspected that pyriboles were altered by nonstoichiometric processes producing "leached-layers" that inhibit diffusion and control weathering rates. These notions have been partly dispelled (e.g., Schott and Berner, 1983) and it is clear that pyribole dissolution rates are functions of complex sets of variables intrinsic and extrinsic to the reacting crystals (Grandstaff, 1986; Eggleston *et al.*, 1989).

Fe and Al show a range of mobilities during pyribole weathering. Consider, for example, the transport distances implicit in the studies of Eggleton (1975), Velbel (1989), and Siever and Woodford (1979). Eggleton (1975) showed that hedenbergite alters to nontronite by a transformation process and suggested that the closeness of the lattice match between the parent and transformed product affects the alteration rate. Iron in the hedenbergite is oxidized but unmobilized as the transformation occurs. Velbel (1989) showed hornblende can be dissolved congruently, with Fe and Al mobilized on the microscale to produce pendants and microboxworks within the parent hornblende grains. Siever and Woodford (1979) showed experimentally that iron can be dissolved from hypersthene, transported and oxidized in solution, and ultimately reprecipitated on neighboring grains as "$Fe(OH)_3$."

Velbel (1989) has provided a good description of characteristic textures developed on weathered amphibole grains in saprolite from the Carroll Knob mafic complex in the Blue Ridge Mountains of North Carolina. Denticulated terminations, paired ferruginous microboxworks (e.g., Stoops *et al.*, 1979), and ferruginous pendants projecting into micro-vuggy pore space are present. Kaolinite, gibbsite and goethite (in possible topotactic relationships with the parent hornblende) are also formed in the saprolite. Velbel (1989) used petrographic and mass balance considerations to conclude that pendants, gibbsite, and the 1:1 phyllosilicate were produced by congruent dissolution and incongruent reprecipitation in an environment characterized by intense leaching with solutions undersaturated with respect to 2:1 clays.

Hornblende denticulation size varies logarithmically with age and burial depth in a soil horizon. Measuring hornblende denticulation size has proven useful for making quantitative estimates of weathering rates in arctic and alpine soils, tills, and periglacial deposits (Locke 1979, 1986; Hall and Martin, 1986; Hall and Michaud, 1988). Denticulations and similar weathering features can develop on both amphibole and pyroxene grains (e.g., Berner and Schott, 1982), but it has never been demonstrated that pyroxene denticulation size is a quantifiable measure of the weathering process.

Chlorite can be transformed to vermiculite when the hydroxide sheet is disrupted by thermal dehydroxyl-

ation or low-temperature acid leaching (Ross and Kodama, 1974; Bain, 1977; Proust *et al.*, 1986; Wilson, 1986). The removal of iron from the chlorite hydroxide sheet is an essential part of the process, and a high iron concentration in the hydroxide sheet appears to be a necessary prerequisite for chlorite vermiculitization. The iron can be oxidized (Makumbi and Herbillon, 1972; Ross, 1975) or unoxidized (Proust *et al.*, 1986) by the vermiculitization process, and sedimentary goethite is sometimes reported as a reaction product (Anand and Gilkes, 1984).

Chlorite vermiculitization can produce an interstratified chlorite/vermiculite (C/V) intermediary phase (Coffman and Fanning, 1975; Anand and Gilkes, 1984; Proust *et al.*, 1986). Interstratified (C/V) is very common (Ross and Kodama, 1976), but it is not a universally observed reaction product. Experiments using brominated water (Ross, 1975; Ross and Kodama, 1974, 1976) show that the iron concentration in the chlorite parent is a key determinant to the reaction products produced by vermiculitization. These experiments show specifically that high-Fe chlorites (diabantite, 2.89 Fe^{2+} per $O_{10}(OH)_8$ structural unit) alter rapidly to discrete vermiculite without forming interstratified C/V intermediaries, that intermediate-Fe^{2+} chlorites (brunsvigite, 1.14 Fe^{2+} per $O_{10}(OH)_8$ structural unit) alter to interstratified C/V, and low-Fe^{2+} chlorites (sheridanite, 0.39 Fe^{2+} per $O_{10}(OH)_8$ structural unit) are weathering-resistant. However, the boundaries are not strictly defined and, for example, Anand and Gilkes (1984) have reported a high-Fe chlorite (ripidolite, 2.26 Fe^{2+} per $O_{10}(OH)_8$) that altered to an interstratified C/V and goethite.

Vermiculites can develop hydroxy-Al interlayers that displace the normal, hydrated, interlayer cations. Hydroxy-Al vermiculites have lowered CEC, reduced expandability, and show inconsistent collapse upon heating or K-saturation. Hydroxy-Al vermiculites form by intense weathering under acid conditions and are stable with respect to vermiculite (and possibly kaolinite) in many weathering horizons (Douglas, 1977). However, there are some exceptions and April *et al.* (1986) suggested that organic acids from leaf litter, or the establishment of more aggressive weathering regimes, had remobilized hydroxy-Al interlayers producing vermiculite in an Adirondack soil.

Periglacial sand dunes were formed ca. 13,000 b.p. in northeastern Indiana. The dunes have a well-documented origin and are being actively weathered under well-defined conditions. Constituent minerals include orthopyroxene, chlorite, vermiculite and hydroxy-Al vermiculite. The dunes present an opportunity to describe and characterize processes related to the weathering of these minerals within a special sedimentary environment. This study has three goals. One, to evaluate the tendency for iron to remain conserved on the microscale in pyroxenes weathered in the sand dune environment. Two, to determine whether orthopyroxenes develop the same quantifiable features as those developed on amphiboles in periglacial tills and arctic soils. Three, to describe and characterize the materials and processes involved in the weathering and vermiculitization of chlorite in a sand dune environment.

SITE DESCRIPTION

The study site is a field of aeolian sand dunes on the Indiana University-Purdue University campus in Fort Wayne, Indiana (IPFW). The dune field occupies an area of about 2.25 ha, rises about 11 m above the adjacent St. Joseph River and crests between 3 and 4 meters above the surrounding till plain.

The dunes date to the Late Pleistocene and were formed by the aeolian reworking of St. Joseph River sediment. During the Late Pleistocene the river was receiving sediment and runoff from receding glaciers. During the winter, flow rates were sufficiently decreased to permit the aeolian reworking of these sediments. Similar dunes occur elsewhere in Allen County and Indiana on the downwind side of rivers (Franzmeier, 1970; Sunderman, 1987). The exact age of these periglacial dunes is unknown. However, it has been suggested that dunes at the Fox Island complex in Allen County were formed ca. 13,000 years ago (Bleuer and Moore, 1978) and a similar age is reasonable for the IPFW dunes.

A lower till of Tazewell or early Woodfordian age and an upper till of Cary or late Woodfordian age (Bleuer, 1974) provided the source for the fluvial sediments that were later reworked into dunes. These tills are 40 m thick in the vicinity of the IPFW campus and contain a combination of local bedrock and crystalline materials from Michigan and the Canadian Shield (Bleuer and Moore, 1978). Locally exposed bedrock includes limestones and dolomites of the Devonian Traverse and Detroit River Formations and the Silurian Wabash and Louisville Formations. There are other, nonexposed, Paleozoic and Precambrian rocks in the subsurface.

The dunes are currently covered with grass but may have once supported hardwood trees. There has been bioturbation of the sediment due to woodchuck activity and the surface was once disturbed by farming. The region receives an annual average of 87 cm of precipitation (NOAA, 1978), and incident rain mostly infiltrates the porous and permeable sands in the dune field.

METHODS

Shelby tubes and an auger were used for near-continuous sampling in the upper 2.8 m of the dune. A split-spoon and auger provided spot sampling from 2.8 to 6.5 m. Shovelled and hand-augered holes supplemented the near-surface sampling. The split-spoon was lost when it got stuck in a clay-rich layer at 2.8 m. Subsequent sampling in the interval from 2.8 to 3.2 m

provided very poor retrieval and, to recover enough material for analysis in this clay-rich layer, it was necessary to take a sample from the flutes of the auger. This sample may have contained sediment from above or below the clay interval. The depth distribution of the samples used for various analyses is indicated in Figure 1.

Samples for X-ray diffraction (XRD) were prepared by suspending 50–100 g of the bulk material in water, dispersing it with an ultrasonic disaggregator, separating the coarse material by gravity sedimentation, removing the <2-μm fraction with a pipette, resonicating the fine fraction and transferring it to a glass slide with a hypodermic syringe. These oriented mounts were dried overnight at room temperature. XRD patterns were subsequently prepared with a Philips APD-3520 XRD system using Cu radiation, graphite monochromator, theta-compensating slit and step scans having effective scan speeds of 0.005–0.02°/s. XRD data were digitally processed and smoothed with a 15-point weighted moving average. Glycolation, glyceration, Mg- and K-saturation, heat treatment, and acid digestion in 1 N HCl were methods used as needed to differentiate among the various clay minerals in the samples.

Petrographic studies were completed on bulk and heavy mineral grain mounts and on thin sections cut from grain mounts fixed in polyester casting resin. Some sections were stained for plagioclase and K-feldspar. Scanning electron microscopy of hand-picked pyroxenes and amphiboles was completed with an ISI Supermini SEM.

Pyroxene etching was quantified by measuring the size of the denticulated terminations that formed as the result of weathering. At least 25 orthopyroxene grains were evaluated from each sample. Greater numbers of grains could not be routinely and easily isolated owing to the limited sample sizes available from the augered holes. The methods follow those previously developed for amphibole grains by Locke (1979, 1986) and Hall and Martin (1986).

Crystalline and noncrystalline iron was quantitatively extracted from the bulk and 63–500-μm fractions using the citrate-bicarbonate-dithionate (CBD) and the acidified ammonium oxalate methods (Schwertmann, 1964; Landa and Gast, 1973; Jackson, 1979). The CBD method dissolves both crystalline and noncrystalline iron oxides and hydroxides (including goethite) but leaves Fe-silicates intact. The oxalate extraction conducted in darkness removes noncrystalline and poorly crystalline iron oxyhydroxides (e.g., ferrihydrite), but does not dissolve the better-crystallized forms. The concentration of iron in the extractions was determined using atomic absorption spectrophotometry (AAS). The samples and standards were carefully matrix-matched to avoid possible signal suppression from the citric acid, although no AAS signal suppression of the citrate-containing samples and standards was noted.

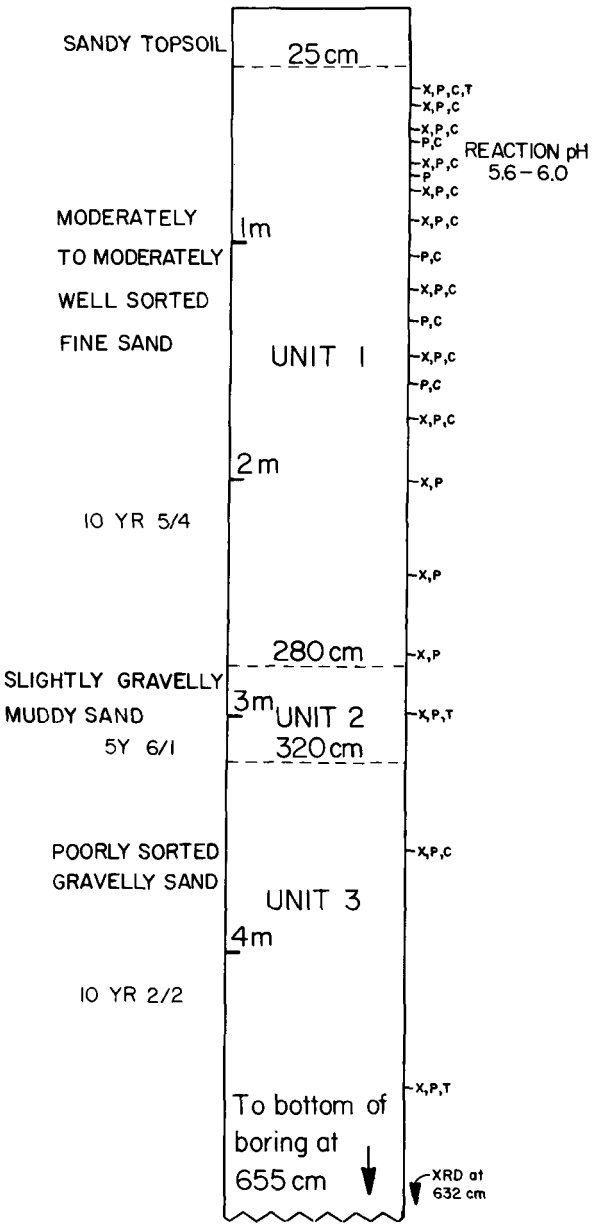

Figure 1. Schematic representation of the borehole from the IPFW dune. Textural names and colors of the sediment are given on the left. The samples used for X-ray diffraction (x), petrographic (p), chemical (c) and textural analysis (t) are indicated on the right. The location of the sample in unit 2, and the upper and lower contacts of unit 2, are poorly constrained.

The relationship between grain size and grain density was determined for the 63–500-μm fraction of the 40 cm deep sample. Acetone-adjusted tetrabromoethane and methylene iodide were used to isolate eight fractions having density ranges of <2.65, 2.65–2.71, 2.71–2.84, 2.84–2.97, 2.97–3.08, 3.08–3.20, 3.20–3.33 and >3.33 g/cm^3. Between 100 and 120 grains from each density interval were photographed and the images

https://doi.org/10.1346/CCMN.1991.0390608 Published online by Cambridge University Press

Table 1. Textural characteristics of the dune.

	Unit 1	Unit 2	Unit 3
Median diameter	0.22 mm (2.17 ϕ)	0.13 mm (2.95 ϕ)	0.52 mm (0.95 ϕ)
Standard deviation	0.72 ϕ[1]	2.00 ϕ[2]	1.87 ϕ[1]
Gravel	0.0%	4.0%	19.9%
Sand	97.6%	57.5%	76.4%
Silt and clay	2.4%	38.5%	3.7%
Name	Moderately to moderately-well sorted fine sand	Poorly to very poorly sorted, slightly-gravelly muddy sand	Poorly-sorted gravelly sand

[1] Inclusive graphic standard deviation.
[2] Graphic standard deviation.

projected and traced onto paper. The tracings were cut from the paper. The cross-sectional area of each grain was determined by weighing the tracings and comparing it to the paper weight of a known area. The average cross-sectional area of the grains in each interval was calculated from these data.

RESULTS

Sediment texture

The sediments penetrated by the boring are divided into three textural units: a fine sand (unit 1), a slightly gravelly, muddy sand (unit 2) and a gravelly sand (unit 3; Figure 1, Table 1). Thicknesses for these units at the dune crest are estimated to be 2.8 m, 0.4 m and 3.35+ m, respectively. The positions of the upper and lower contacts of unit 2 are not exactly known because of the poor recovery in the interval. Unit 1 comprises the aeolian portion of the dune and is formed from sediment reworked from the adjacent St. Joseph River. Units 2 and 3 have textures that suggest a subaqueous origin, and these units may have formed as overbank and point bar/channel sediments. All three units are derived from the same source.

There is a statistical correlation between the grain size and grain density of the unit 1 sands (Figure 2). This correlation reflects the aeolian sorting and the best-fit curve to the data closely matches a simple Stokes' law settling curve for grains in air. The 2.78 and 2.90 g/cm^3 fractions have large standard deviations and do not conform to either the statistical or theoretical relationships established by the other density splits. These fractions are sparsely populated, are skewed to the larger sizes, and are comprised dominantly of quartz and feldspar with opaque coatings removable by CBD extraction. This suggests that these are quartz and feldspar grains transported in hydraulic equilibrium and modified after deposition by the addition of organic and ferroan coatings.

Coarse-grain mineralogy

The 63–500-μm fraction of unit 1 has an average composition of 57% quartz, 15% K-feldspar, 11% rock fragments and polycrystalline quartz, 10% plagioclase feldspar, 4% chert, 1% almandine garnet, 1% amphibole, and <1% each of pyroxene and biotite. The sand-sized mineralogies of units 2 and 3 are similar to the mineralogy of unit 1 except for the presence of 2–5% calcite and trace dolmite. Carbonate-bearing rock fragments are present in units 2 and 3, but do not occur in unit 1 (Table 1).

The most common pyroxene is an orthopyroxene of hypersthene-bronzite composition having parallel extinction, moderate pleochroism between pale pinkish-red and apple-green, moderately low birefringence, positive elongation, and 2V about 60°. The diagnosis of an orthopyroxene composition was confirmed by X-ray diffraction of several hand-picked grains.

The most common amphibole is a hornblende that is deeply colored, strongly pleochroic from moderate to deep green, optically negative, 2V of 60–70°, and

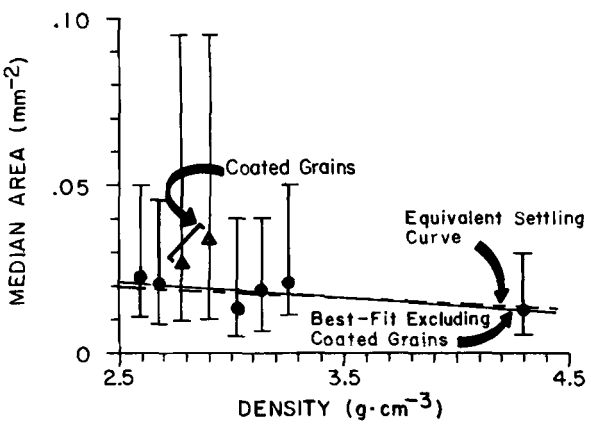

Figure 2. Grain size versus density for the 63–500-μm fraction of unit 1. Bars denote the range between the largest and smallest grain size present in the fraction. The size-density relationship closely follows the line predicted by Stokes' law settling of grains in air. The fractions with densities of 2.78 and 2.90 g/cm^3 are comprised dominantly of quartz and feldspar having opaque overgrowths and were probably modified after deposition. Note the large size range for the 2.78 and 2.90 g/cm^3 fractions.

https://doi.org/10.1346/CCMN.1991.0390608 Published online by Cambridge University Press

maximum extinction angles of 22°. Good XRD patterns were obtained, and analysis shows this amphibole has cell dimensions of a = 9.88 Å, b = 18.07 Å, c = 5.33 Å, β = 105.11°.

Groundwater pH

Unit 1 is a part of the Plainfield soil series and has sediment characterized by high permeability (12.7–25.4 cm/hr) and low reaction pH (5.6–6.0; Kirschner and Zachary, 1969). In contrast, the groundwater from unit 3 is alkaline and has a measured pH of about 7.55. This alkaline water can be occasionally introduced to unit 1 when heavy rains saturate the ground and raise the local water table.

Pyroxene etching

The pyroxenes are etched by weathering, and many of the weathering features previously noted in experimental and natural systems are seen here (e.g., Berner *et al.*, 1980; Berner and Schott, 1982; Velbel, 1989). Indeed, it is remarkable how the microscopic appearance of these orthopyroxenes weathered in a periglacial sand dune and derived from glacial till so closely approximates the appearance of the orthopyroxenes from areas unaffected by Pleistocene glaciation (Berner and Schott, 1982).

Weathering apparently starts with the development of small, cleavage-parallel etch pits on {010} and {100} surfaces (Figures 3a, b). These pits are not always developed equally on all faces and grains were observed where one form was smooth and the other was heavily etched. Denticulations develop when the pits coalese and crop out on the basal surfaces (Figures 3c–e). The denticulations are crystallographically oriented along the z-axis and the flat sides of the denticulations are layered parallel to {100}. Sheet features are genetically related to denticulations but appear as laminae parallel to {100} without the well-developed sawtooth terminations (Figure 4). The origin of the sheet features and the denticulations are both attributable to the presence of exsolution lamellae in the (100) plane (Berner and Schott, 1982).

Cave features are pits that form at high angles to the z-axis (Figure 5) and contain denticulations that project into the interior space. Cave features deepen by an incremental process with a step-size similar to the thickness of the sheets seen in Figure 4. The SEM photographs carry insufficient information to determine unambiguously all aspects of crystallographic orientation, but petrographic examination of grain mounts suggests the cave features may form preferentially on the (100) face. If so, the presence of lamellae in {100} may explain the step-wise growth of the cave features.

A curious aspect of the cave features is that they sometimes occur periodically along the z-axis (Figure 5b), which is reminiscent of the repetitious occurrence of etch pits previously seen in augite grains (Berner and Schott, Pl. 1d, 1982). Brookite and ilmenite may occur as inclusions on {001}, however, {001} does not correspond to a direction that commonly develops exsolution lamellae. The periodicity is, at present, an unexplained phenomenon and should be reexamined at a future date.

Ferruginous microboxworks and pendants like those described by Velbel (1989) were not observed in this system. Some grains had surface overgrowths that are probably part of the ferruginous material removable with oxalate and CBD extractions.

The mean orthopyroxene denticulation size decreases with increasing sample depth (Figure 6). The decrease follows a well-correlated logarithmic trend throughout the upper 3 meters (i.e., in unit 1). Below 3 m there is an abrupt decrease in the denticulation size to a "zero-value" of about 0.45 μm; so-called because the least-weathered material seems always to have at least this much etching and is apparently characteristic of unweathered orthopyroxene grains (e.g., Locke, 1979). The best-fit curve extrapolated to 0.45 μm shows that the "zero-value" would have been reached at a depth of about 10 m if the discontinuity did not exist. The placement of the discontinuity cannot be determined exactly because of the poor sampling in the 2.8–3.2 m range. It probably occurs somewhere within the unit 2 lithology.

There is no well-correlated relationship between denticulation size and sample depth for the amphibole grains. Several factors could be responsible: (1) the possibility that previously-etched amphiboles were inherited from the source, (2) that slower amphibole etching rates increased the relative importance of measurement errors, (3) that slower etching rates placed the zone of most-active amphibole etching entirely at the shallower depths most disturbed by bioturbation, or (4) that the range in amphibole compositions was sufficient to cause different amphiboles to etch at different rates.

X-ray diffraction

There are two different clay-fraction assemblages (Table 2; Figures 7 and 8). The first extends from the surface to a depth of about 300 cm and comprises textural unit 1 and part of unit 2. The second extends from about 300 cm to the bottom of the boring and comprises part of textural unit 2 and unit 3. The upper assemblage contains vermiculite and scattered smectite and goethite. The lower assemblage contains chlorite and small concentrations of calcite and dolomite. Kaolinite, illite, quartz, plagioclase feldspar and K-feldspar occur in both clay-fraction assemblages.

Diffraction patterns were obtained from unoriented mounts of the $<$10-μm fraction at 632 cm for the purpose of evaluating the chlorite composition. The relative intensities of the chlorite 002, 003, 004 and 005 peaks are 85, 17.5, 100 and 10, respectively. These

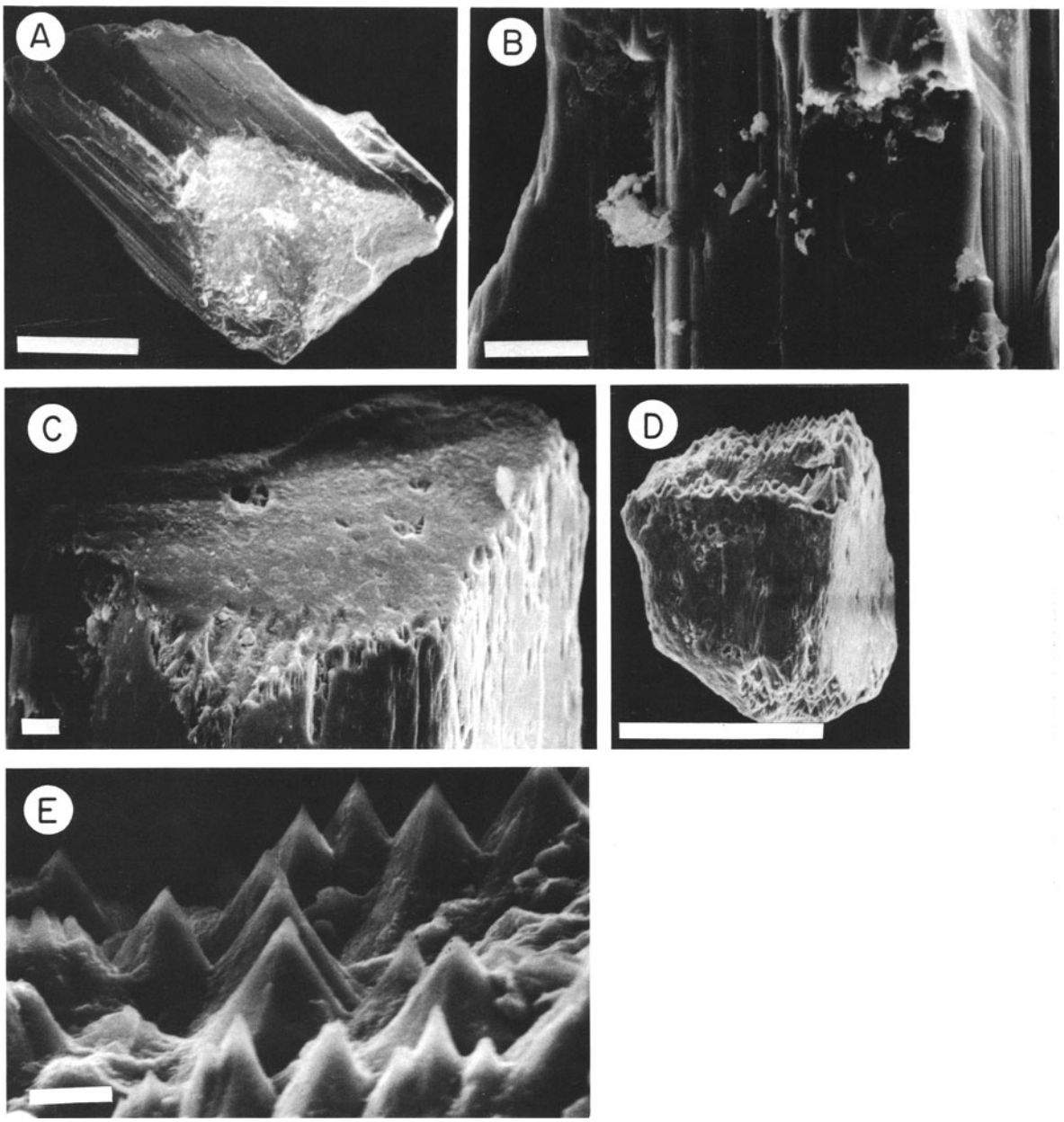

Figure 3. Steps in the development of pyroxene denticulations. (A) Fresh pyroxene grain. (B) Small etch-pit oriented parallel to the *z*-axis. (C) Etch-pits terminating at the basal pinacoid. (D) and (E) Heavily denticulated grains. Scale bars = 250 μm in A and D, and 10 μm in (B), (C) and (E).

data correspond to an iron-rich chlorite having an approximate composition of $(Mg, Al)_2Fe_4(Si, Al)_4O_{10}(OH)_8$, and an octahedral-to-tetrahedral iron ratio of 2.45:1.55 (Brown and Brindley, 1980; Moore and Reynolds, 1989).

The vermiculite from below 64 cm has d_{001} at about 14.3–14.5 Å when air-dried, 14.1 Å when glycerated, 15.2–15.5 Å when ethylene glycolated, 10.1–10.2 Å when heated to 375°C, and 10.1–10.2 Å when K-saturated (Table 3; Figure 9). The collapse with heat and with K-saturation is complete and produces a peak that overlaps or forms a doublet with the illite (002). The peak collapsed by heating could be partially rehydrated with exposure to the air, but collapse by a combination of K-saturation and heating to 300°C was permanent. The vermiculite (001) could not be reexpanded after this treatment, either in the air or with glycerol.

The vermiculite from above 64 cm has d_{001} at about 14.3 Å when air-dried, 14.1 Å when glycerated, 14.4–

https://doi.org/10.1346/CCMN.1991.0390608 Published online by Cambridge University Press

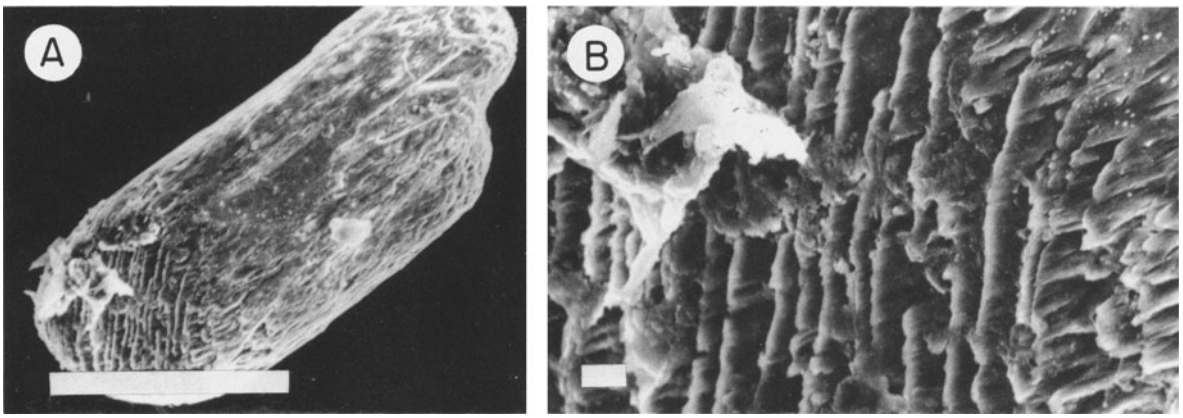

Figure 4. Etching sometimes results in the formation of sheet-like features along the {100} parting. The cave features in Figure 5 deepen in a stepwise fashion dependent on these parting thicknesses. Scale bar = 250 μm in (A) and 10 μm in (B).

14.5 Å when ethylene glycolated. The (001) peak was incompletely collapsed by heat and K-saturation (Table 3; Figure 9). Heating to 375°C produced a broad peak with a center at about 12.1 Å, and K-saturation produced a very broad, asymmetric peak with a shoulder at about 13.9 Å. This vermiculite could also be partially rehydrated after heating and could not be reexpanded with glycerol after a combination of K-saturation and heat treatment.

Soluble iron

The iron extracted from the bulk and the 63–500-μm fractions is shown in Figure 10. As expected, CBD-extractable iron exceeds oxalate-extractable iron in all samples, and the ratio between oxalate- and CBD-extractable iron is nearly constant throughout the dune sand. The peak in the extractable-iron concentration at 66–77 cm corresponds to the depth where goethite is first detected by XRD (Table 2). Interestingly, extractable-iron in the bulk samples exceeds the extractable iron in the 63–500-μm fraction by factors between 2 and 5. This result is significant as only 2.4% of the total sediment in unit 1 falls outside the 63–500-μm fraction, and it is clear that extractable iron is preferentially concentrated in the finer grain sizes.

DISCUSSION

Carbonate removal

Unit 1 was derived from local fluvial sediments reworked by subaerial processes. Unit 3 was derived from the same source reworked by subaqueous processes. Carbonate grains of a size that would have sorted with the aeolian sands (Figure 2) are present in unit 3. This indicates that carbonates were part of the shared source, and were probably once a part of the unit 1 (aeolian)

Table 2. Mineralogy of the <2-μm fraction.

Depth (cm)	Qtz	Spar	Ill	Kaol	Verm	Smec	Chl	Cc	Dol	Goeth
33	P	P	P	P	P	—	—	—	—	—
40	P	P	P	P	P	—	—	—	—	—
51	P	P	P	P	P	—	—	—	—	—
64	P	P	P	P	P	—	—	—	—	P
76	P	P	P	P	P	—	—	—	—	P
89	P	P	P	P	P	T	—	—	—	P
119	P	P	P	P	P	T	—	—	—	P
147	P	P	P	P	P	T	—	—	—	P
173	P	P	P	P	P	—	—	—	—	P
200	P	P	P	P	P	P	—	—	—	T
240	P	P	P	P	P	P	—	—	—	P
300	P	P	P	P	T	—	P	P	—	—
358	P	P	P	T	—	—	P	P	P	—
457	P	P	P	T	—	—	P	P	P	—
632	P	P	P	P	—	—	P	P	P	—

Symbols: P = present; T = trace; — = not detected; Qtz = quartz; Spar = feldspar; Ill = illite; Kaolite = kaolinite; Verm = vermiculite; Smec = smectite; Chl = chlorite; Cc = calcite; Dol = dolomite; Goeth = goethite.

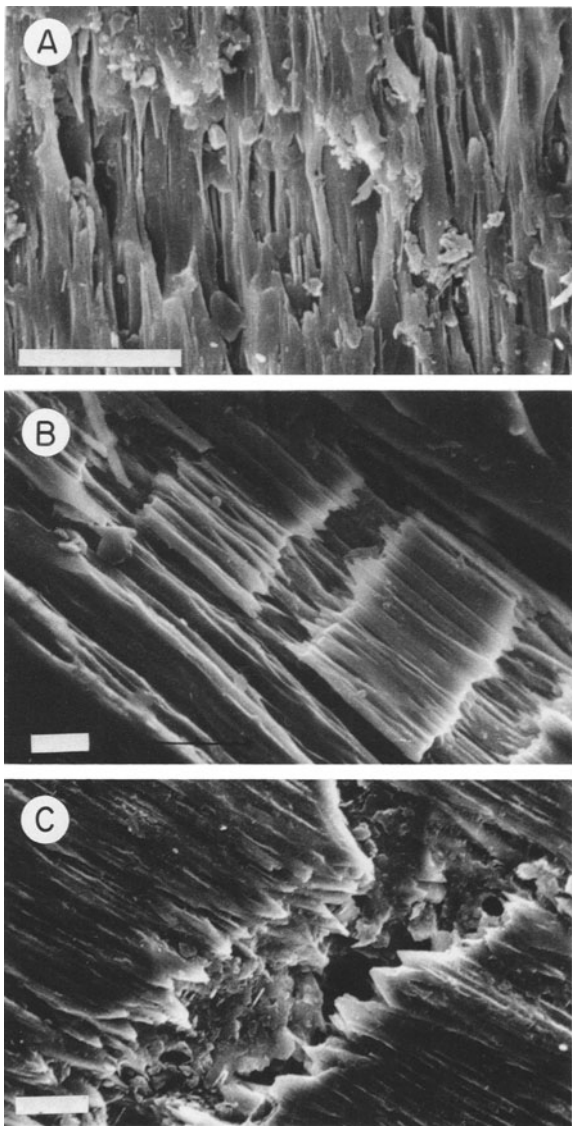

Figure 5. Cave features. Lateral coalescence of etch-pits leads to the formation of cave features. These cave features are oriented at high angles, and are frequently regularly spaced along the z-axis. Scale bars = 10 μm.

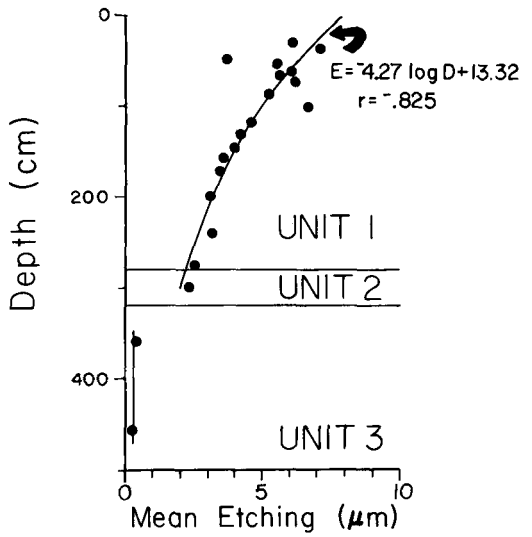

Figure 6. Relationship between sample depth and the mean etch-depth of the denticulations formed on orthopyroxenes in the IPFW dune. Etching follows a well-correlated decrease with increasing depth in the core. Scatter in the upper meter is attributable to the smearing effects of bioturbation. The etching "zero-value" is abruptly reached in the carbonate-bearing sediments. The "zero-value" would have been reached at a depth of about 10 m in the absence of this discontinuity.

sands. The current absence of carbonates in unit 1 is attributable to dissolution by weathering solutions, reflecting the acidic and well-drained conditions prevalent in the upper 2.8 m of the dune.

Pyroxene etching

The pyroxene denticulation size decreases with increasing depth in the dune (Figure 6). The trend is smooth and logarithmic throughout unit 1, but becomes discontinuous where the sediment turns clay- and carbonate-rich (Figure 6). This discontinuity is attributable to the slower weathering rates characteristic of the more alkaline conditions that begin in unit 2 and exist throughout unit 3.

Figure 11 shows the etch-depth profile for the dune pyroxenes compared to similar profiles for amphiboles in alpine soils from southwestern Montana and arctic soils and tills from Baffin Island in the Northwest Territories of Canada. The pyroxene etching is faster and more complete, and the zero-value is deeper in the dune (it would be about 10 m in the absence of the discontinuity) than it is for the soils and tills. There are three possible explanations for these differences. One, pyroxenes are inherently less stable than amphiboles in surface environments and are more rapidly

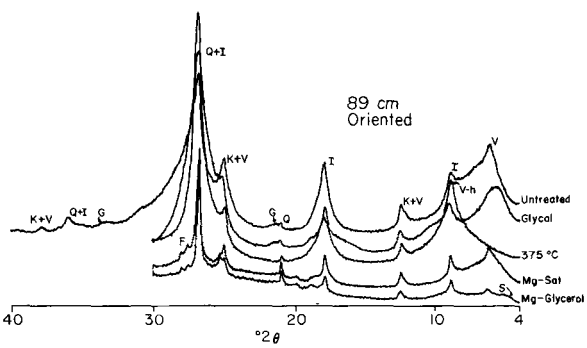

Figure 7. XRD patterns for oriented samples from 89 cm depth. Symbols: V = Vermiculite; V-h = Vermiculite heated to 375°C; I = Illite; K = Kaolinite; Q = Quartz; G = Goethite; S = Smectite; F = Feldspar.

https://doi.org/10.1346/CCMN.1991.0390608 Published online by Cambridge University Press

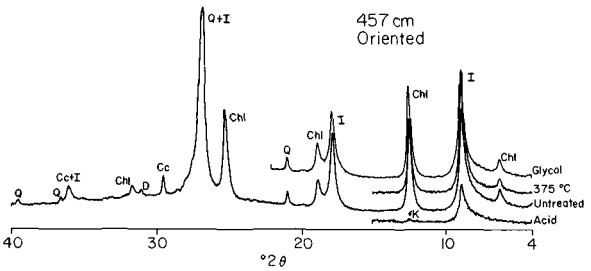

Figure 8. XRD patterns for oriented samples at 457 cm depth. Symbols: Chl = Chlorite; Cc = Calcite; D = Dolomite; other symbols as in Figure 7.

and completely disintegrated by weathering processes. Two, the aeolian dune sands are highly permeable, have low reaction pH and low buffering capacity; characteristics that permit rapid penetration of potent weathering solutions and result in a greater "zero-value" depth. Three, there are some significant climatic differences among the study areas. Baffin Island has a mean annual temperature of −10°C, and 30 cm of liquid-equivalent precipitation falls each year (Locke, 1979). Southwestern Montana has a mean annual temperature of 4.8°C, and 36.6 cm of annual precipitation (NOAA, 1978). Allen County has a mean annual temperature of 9.9°C, and an annual average of 86.9 cm of precipitation (NOAA, 1978). Despite these differences, the profiles are generally similar and pyroxenes, like amphiboles, produce quantifiable etch-depth curves.

Schott and Berner (1985) calculate that the silica release-rate from bronzite decreases by a factor of four if the pH rises one unit (in the pH range of 1–6). There is about a three-fold decrease in the etching rate of the orthopyroxenes between the top and bottom of unit 1. This modest decrease in the etch-rate can be explained

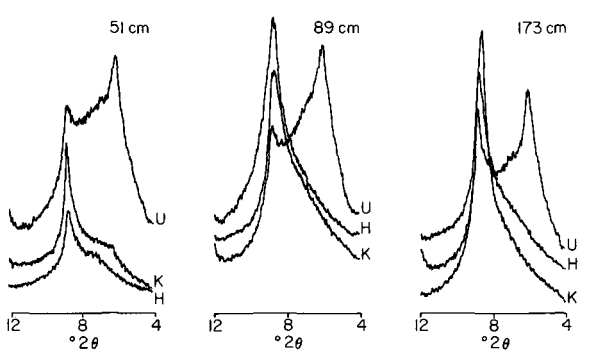

Figure 9. XRD patterns showing the position of the vermiculite 001 peak for samples that are untreated (U), K-saturated (K), and heated to 375°C (H). The vermiculite from depths shallower than 64 cm is characterized by incomplete collapse after heating and K-saturation, and is a hydroxy-Al variety.

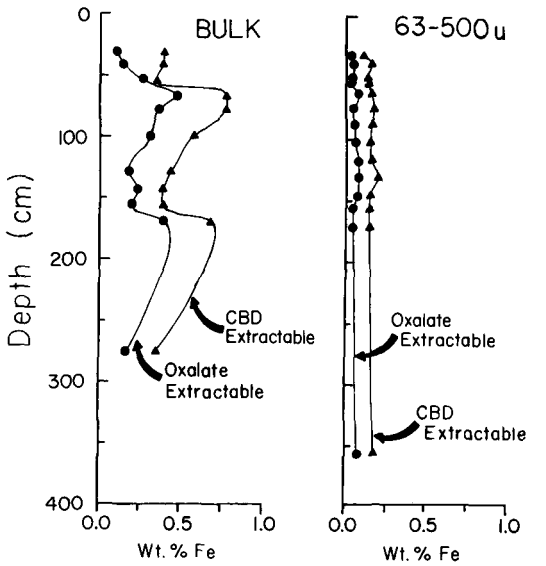

Figure 10. Concentrations of iron extractable with the CBD and oxalate methods. Most of the extractable-iron is in the <63-μm fraction, even though the finer grain sizes account for only 2.4% of the total sediment. The peak in the extractable-iron concentration at 64 cm corresponds to the first occurrence of goethite and the boundary between vermiculite and hydroxy-Al vermiculite varieties.

by only a slight rise in pH as rain water passes downward through the dune and even occasionally mixes with alkaline groundwater introduced from below. There is no reason to suspect a more complicated mechanism exists for controlling the etch-rate of the dune pyroxenes.

In his study of amphibole weathering, Velbel (1989) concludes that it is unnecessary to invoke leached layers to explain nonstoichiometry in hornblende weathering reactions. There is nothing in the present study to suggest that this conclusion is not equally applicable to the dune pyroxenes. There are, however, some interesting differences in the mobility and retention of iron and other "immobile" elements in the two systems. Velbel (1989) shows that Fe, Al and some Si are conserved within hornblende weathering microenvironments producing oriented pendants and microboxworks within the grains. Conversely, the dune pyroxenes show no pendants, no microboxworks, and goethite is not enriched in the pyroxene-bearing fraction. These observations imply that the transport-lengths of the "immobile" elements are greater for the dune pyroxenes than for Velbel's amphiboles, and that transformation and topotactic replacement of mineral surfaces are unimportant processes in the alteration of these pyroxenes.

Chlorite vermiculitization

Chlorite and vermiculite have antipathetic distri-

https://doi.org/10.1346/CCMN.1991.0390608 Published online by Cambridge University Press

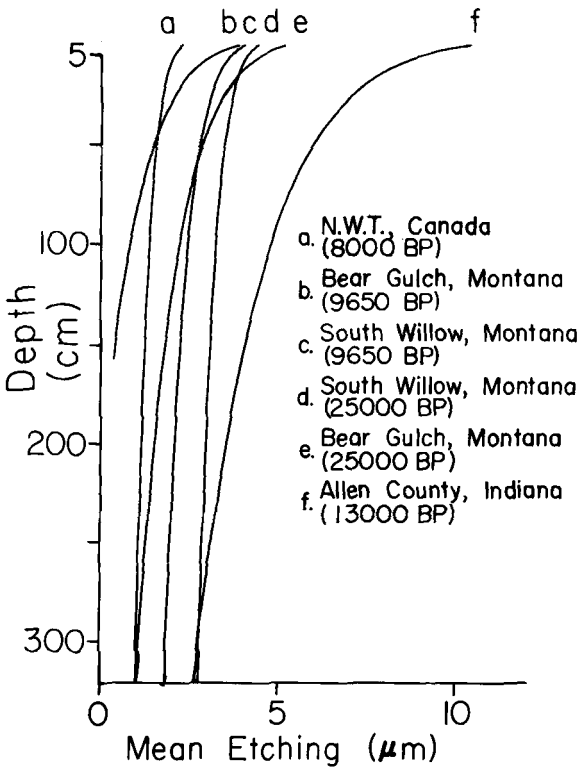

Figure 11. Relationship between sample depth and the mean etch-depth of the denticulations formed on amphiboles from the Northwest Territories and Montana, and on orthopyroxenes from the IPFW dune. Amphibole data from Locke (1986) and Hall and Martin (1986).

butions (Table 2) and it is apparent that chlorite has been altered to vermiculite by weathering processes. Goethite occurs between 64 and 240 cm depth (Table 2). Extractable-iron concentrations range as high as 0.75 wt. % Fe in this interval (Figure 10). These distributions of goethite and extractable iron are probably due to the downward accumulation of iron released from weathered chlorite. The increased concentration of iron and other leached ions at depth, combined with an increase in average pH, are also probably responsible for the sporadic formation of small concentrations of smectite below 89 cm (Table 2). The possibility that kaolinite is forming above 89 cm cannot be evaluated because of the interference from the detrital kaolinite found throughout the dune.

The XRD results indicate that the vermiculite has a layer charge greater than or equal to 0.63 per $O_{10}(OH)_8$ structural unit and that this is a vermiculite in the strict sense defined by the AIPEA (Malla and Douglas, 1987). There are, however, two different types of vermiculite in the dune. The vermiculite from depths below 64 cm expands to 15.5 Å when ethylene glycolated and fully collapses when heated or K-saturated. The vermiculite from depths above 64 cm expands only to 14.4 Å when ethylene glycolated and is only partially collapsed by K-saturation and heating. These results indicate the presence of vermiculite below 64 cm and a hydroxy-Al vermiculite at the shallower depths.

Acidic conditions tend to favor the development of hydroxy-Al interlayers in the vermiculites from surface horizons (Douglas, 1977), but there are exceptions to the rule that are sometimes explained by the type of acid that dominates the weathering solution (Vicente *et al.*, 1977). For example, vermiculite forms in the A horizon at the same time hydroxy-Al vermiculite forms in the deeper B horizons of certain Adirondack soils (April *et al.*, 1986). This distribution can be explained by the presence of organic acids (especially citric and oxalic acids formed under aerobic conditions) from the overlying leaf-litter that prevent the formation of hydroxy-Al interlayers in the vermiculites at near-surface depths (Vicente *et al.*, 1977; April *et al.*, 1986).

In the dune, the hydroxy-Al vermiculite occurs nearest the surface, which is consistent with the dominant role played by carbonic acid in this sandy, organic-poor sediment (Vicente *et al.* 1977). The transition from hydroxy-Al vermiculite to vermiculite occurs at 64 cm depth. This corresponds to the first appearance of goethite and a spike in the accumulation of extractable-iron in the finer grain fractions (Table 2; Figure 10). Interestingly, this depth does not correspond to an abrupt change in sediment texture, nor does it correspond to an abrupt decrease in the orthopyroxene weathering rate (Figure 6). The correspondence raises an interesting set of questions about the source of aluminum for the hydroxy-Al interlayers (Vicente *et al.*, 1977). Hydroxy-Al can be derived (in the solid state) from the chlorite, or it can be precipitated from an aqueous species derived from the simultaneous weathering and dissolution of associated feldspars (see, e.g., Holdren and Berner, 1979). The latter would seem to be more sensitive to the types of controls that regulate iron mobility, but I do not have a specific explanation for the correspondence between the appearance of goethite and the transition between vermiculite and hydroxy-Al vermiculite. These two distinct events may be merely coincidental.

Table 3. 001 spacing (Å) for vermiculite.

Treatment	51 cm	89 cm	173 cm
Air-dry	14.3	14.5	14.5
Mg-saturated	14.1	14.3	—
Ethylene glycol	14.4	15.4	15.2
Mg-saturated + glycerol	14.1	14.1	—
Heated 375°C[1]	12.1[2]	10.2	10.1
K-saturated	13.9[3]	10.2	10.1

— Not determined.
[1] Could be partially rehydrated with exposure to air.
[2] Broad.
[3] Shoulder extending to higher angles.

https://doi.org/10.1346/CCMN.1991.0390608 Published online by Cambridge University Press

Interstratified chlorite/vermiculite (C/V) was not identified and is either never formed or too ephemeral to be detected. The experiments of Ross (1975) and Ross and Kodama (1974, 1976) show that the vermiculitization of chlorite is sensitively dependent on the concentration and oxidation of Fe^{2+} in the chlorite parent. In the dune, the parent chlorite is a high-Fe variety, and the field evidence that this chlorite is weathered directly to vermiculite without an interstratified C/V intermediary provides additional field confirmation for the experiments of Ross (1975) and Ross and Kodama (1974, 1976).

SUMMARY

Orthopyroxenes of hypersthene-bronzite composition have been etched by weathering in Pleistocene sand dunes in northeastern Indiana. The process proceeds by a recognizable series of steps that starts with the development of small lenticular etch pits on prism surfaces and continues with the growth of denticulated terminations at the basal ends. The denticulation growth is quantifiable and there is a well-correlated logarithmic curve that relates mean denticulation size to sample depth. The shape of this curve is similar to those previously described for weathered amphiboles. However, the extrapolated depth of the zero-value is deeper for the dune pyroxenes and reflects the greater instability of pyroxenes, the effects of climate, and the high permeability and low buffering capacity of the dune sands.

There are no ferruginous pendants or other indications that iron was conserved on the microscale within the weathered grains. Microvoid space on the surfaces and between the denticulations is produced by congruent dissolution followed by transport of the dissolved iron out of the microenvironment. Redeposition of this iron is ultimately determined by the chemical and physical macroproperties of the sediment.

A high-Fe chlorite has been weathered to a vermiculite with the release of iron and without any evidence of a chlorite/vermiculite intermediary phase. The vermiculite in the upper 64 cm is a hydroxy-Al variety, typical for vermiculites formed in acidic, well-leached, systems. The transition to a hydroxy-Al vermiculite at 64 cm corresponds to the depth where goethite first appears as a weathering product and where there is a spike in the concentration of extractable-Fe in the finer grain sizes. There is presently no explanation for this correspondence and it may be coincidental.

ACKNOWLEDGMENTS

Comments and suggestions by Herman Roberson and Michael Anthony Velbel contributed significantly to the final draft of this report. XRD equipment was purchased with funds provided by NSF grant CSI-8750250.

REFERENCES

Anand, R. R. and Gilkes, R. J. (1984) Weathering of hornblende, plagioclase and chlorite in meta-dolerite, Australia: *Geoderma* **34,** 261–280.

April, R. H., Hluchy, M. M., and Newton, R. M. (1986) The nature of vermiculite in Adirondack soils and tills: *Clays & Clay Minerals* **34,** 549–556.

Bain, D. C. (1977) The weathering of chloritic minerals in some Scottish soils. *Jour. Soil Sci.,* **28,** 144–164.

Berner, R. A. and Schott, J. (1982) Mechanism of pyroxene and amphibole weathering II. Observations of soil grains: *Amer. Jour. Sci.* **282,** 1214–1231.

Berner, R. A., Sjoberg, E. L., Velbel, M. A., and Krom, M. D. (1980) Dissolution of pyroxenes and amphiboles during weathering: *Science* **207,** 1205–1206.

Bleuer, N. K. (1974) Buried till ridges in the Fort Wayne area, Indiana, and their regional significance: *Geol. Soc. Amer. Bull.* **85,** 917–920.

Bleuer, N. K. and Moore, M. C. (1978) *Environmental Geology of Allen County, Indiana:* Indiana Geol. Survey Special Report **13.**

Brown, G. and Brindley, G. W. (1980) X-ray diffraction procedures for clay mineral identification: in *Crystal Structures of Clay Minerals and their X-Ray Identification,* G. W. Brindley and G. Brown, eds., Mineralogical Society Monograph **5,** London, 305–360.

Coffman, C. B. and Fanning, D. T. (1975) Maryland soils developed in residuum from chloritic metabasalts having high amounts of vermiculite in sand and silt fractions: *Soil Sci. Soc. Amer. Proc.* **39,** 723–732.

Douglas, L. A. (1977) Vermiculites: in *Minerals in Soil Environments,* J. B. Dixon and S. B. Weed, eds., Soil Sci. Soc. Amer., Madison, Wisconsin, 259–292.

Eggleston, C. M., Hochella, M. F., Jr., and Parks, G. A. (1989) Sample preparation and aging effects on the dissolution rate and surface composition of diopside: *Geochim. et Cosmochim. Acta* **53,** 797–804.

Eggleton, R. A. (1975) Nontronite topotaxial after hedenbergite: *Am. Mineral.* **60,** 1063–1068.

Franzmeier, D. P. (1970) Particle size sorting of proglacial eolian materials: *Soil Sci. Soc. Amer. Proc.* **34,** 920–924.

Grandstaff, D. E. (1986) The dissolution rate of forsteritic olivine from Hawaiian beach sand: in *Rates of Chemical Weathering of Rocks and Minerals,* S. M. Colman and D. P. Dethier, eds., Academic Press, New York, 41–59.

Hall, R. D. and Martin, R. E. (1986) The etching of hornblende grains in the matrix of alpine tills and periglacial deposits: in *Rates of Chemical Weathering of Rocks and Minerals,* S. M. Colman and D. P. Dethier, eds., Academic Press, New York, 101–128.

Hall, R. D. and Michaud, D. (1988) The use of hornblende etching, clast weathering, and soils to date alpine glacial and periglacial deposits: A study from southwestern Montana: *Geol. Soc. Amer. Bull.* **100,** 458–467.

Holdren, G. R., Jr. and Berner, R. A. (1979) Mechanisms of feldspar weathering—I. Experimental studies: *Geochim. et Cosmochim. Acta* **43,** 1161–1171.

Jackson, M. L. (1979) *Soil Chemical Analysis—Advanced Course,* 2nd ed. Published by the author, Madison, Wisconsin.

Kirschner, F. R. and Zachary, A. L. (1969) *Soil Survey of Allen County, Indiana:* U.S. Dept. of Agriculture, Washington, DC.

Landa, E. R. and Gast, R. G. (1973) Evaluation of crystallinity in hydrated ferric oxides: *Clays & Clay Minerals* **21,** 121–130.

Locke, W. W. (1979) Etching of hornblende grains in arctic soils: An indicator of relative age and paleoclimate: *Quat. Res.* **11,** 197–212.

Locke, W. W. (1986) Rates of hornblende etching in soils on glacial deposits, Baffin Island, Canada: in *Rates of Chemical Weathering of Rocks and Minerals,* S. M. Colman and D. P. Dethier, eds., Academic Press, New York, 129–145.

Makumbi, L. and Herbillon, A. J. (1972) Vermiculitisation experimentale d'une chlorite: *Bull. Groupe franc. Argiles* **24,** 153–164.

Malla, P. B. and Douglas, L. A. (1987) Identification of expanding layer silicates: Layer charge vs. expansion properties: in *Proc. Int. Clay Conf., Denver, 1985,* L. G. Schultz, H. van Olphen and F. A. Mumpton, eds., 277–283.

Moore, D. M. and Reynold, R. C., Jr. (1989) *X-Ray Diffraction and the Identification and Analysis of Clay Minerals:* Oxford University Press, Oxford, 332 pp.

NOAA (1978) *Climates of the States, Vol. 1. Alabama–Montana:* Gale Research Co., Detroit, 606 pp.

Proust, D., Eymery, J.-P., and Beaufort, D. (1986) Supergene vermiculitization of a magnesian chlorite: Iron and magnesium removal processes: *Clays & Clay Minerals* **34,** 572–580.

Ross, G. J. (1975) Experimental alteration of chlorites into vermiculites by chemical oxidation: *Nature* **255,** 133–134.

Ross, G. J. and Kodama, H. (1974) Experimental transformation of a chlorite into a vermiculite: *Clays & Clay Minerals* **22,** 205–211.

Ross, G. J. and Kodama, H. (1976) Experimental alteration of a chlorite into a regularly interstratified chlorite-vermiculite by chemical oxidation: *Clays & Clay Minerals* **24,** 183–190.

Schott, J. and Berner, R. A. (1983) X-ray photoelectron studies of the mechanism of iron silicate dissolution during weathering: *Geochim., et Cosmochim. Acta* **47,** 2233–2240.

Schott, J. and Berner, R. A. (1985) Dissolution mechanisms of pyroxenes and olivines during weathering: in *The Chemistry of Weathering,* J. I. Drever, ed., Reidel, Dordrecht, 35–53.

Schwertmann, U. (1964) Differenzierung der eisenoxide des bodens durch extraktion mit ammoniumoxalat-lösung: *Z. Pflanzenernahr. Dung., Bodenk.* **105,** 194–202.

Siever, R. and Woodford, N. (1979) Dissolution kinetics and the weathering of mafic minerals: *Geochim. et Cosmochim. Acta* **43,** 717–724.

Stoops, G., Altemüller, H.-J., Bisdom, E. B. A., Delvigne, J., Dobrovolsky, V. V., Fitzpatrick, E. A., Paneque, G., and Sleeman, J. (1979) Guidelines for the description of mineral alterations in soil micromorphology: *Pedologie* **29,** 121–135.

Sunderman, J. A. (1987) Fort Wayne, Indiana: Paleozoic and Quaternary geology: in *Centennial Field Guide, Vol. 3. North-Central Section,* D. L. Biggs, ed., Geol. Soc. Amer., Denver, Colorado, 325–332.

Velbel, M. A. (1989) Weathering of hornblende to ferruginous products by a dissolution-reprecipitation mechanism: *Clays & Clay Minerals* **37,** 515–524.

Vicente, M. A., Razzaghe, M., and Robert, M. (1977) Formation of aluminum hydroxy vermiculite (intergrade) and smectite from mica under acidic conditions: *Clay Miner.* **12,** 101–112.

Wilson, M. J. (1986) Mineral weathering processes in podzolic soils on granitic materials and their implications for surface water acidification: *Jour. Geol. Soc. London* **143,** 691–697.

(Received 14 June 1991; accepted 26 September 1991; Ms. 2112)